

Accelerated Corrosion of Carbon Steel by the Galvanic Coupling with Magnetite in Simulated Secondary Water under Flowing Conditions

Geun Dong Song, Soon-Hyeok Jeon, Do Haeng Hur*

Nuclear Materials Research Division, Korea Atomic Energy Research Institute, 989-111 Daedeok-daero, Yuseong-gu, Daejeon, 34057, Republic of Korea

*Corresponding author: dhhur@kaeri.re.kr

1. Introduction

The surface of carbon steel piping is normally covered with protective magnetite layers under reducing operation conditions of pressurized water reactors (PWRs). These layers are rapidly removed by flow accelerated corrosion in the turbulent flow region, and wall thinning of carbon steel piping is accelerated. This type of corrosion is affected by various water chemistry factors. The temperature, dissolved oxygen, and pH affect the stability of magnetite layer, while fluid dynamics affects the mass transfer of soluble iron from the surface of the magnetite layer [1-3].

Although the effects of various water chemistry factors have been evaluated comprehensively, there is another factor that should be considered in evaluating the corrosion of carbon steel piping. When magnetite layers formed on carbon steel are partially removed in areas where turbulence is severe, the exposed metal surface of carbon steel is electrically connected with the remaining magnetite layer. Because magnetite shows almost metallic behavior with respect to electrical properties [4], a galvanic cell between the exposed metal surface of carbon steel and magnetite can be formed under this condition. Recently, it has been reported that the galvanic coupling with magnetite accelerates the corrosion of carbon steel [5,6] and Ni-based alloys [7,8] in various environments. Accordingly, this galvanic coupling is expected to be an additional acceleration factor on the corrosion of carbon steel piping in PWRs. However, the effect of magnetite has still not been considered in evaluating the corrosion of carbon steel in PWRs.

The objective of this work is to investigate the effect of magnetite on the corrosion of carbon steel in simulated secondary water under flowing conditions. To evaluate the corrosion behavior of pure magnetite and its effect, the magnetite specimens were prepared by the electrodeposition method. The galvanic corrosion behavior between carbon steel and magnetite was investigated by using electrochemical and immersion tests. Based on the results, the galvanic coupling with magnetite is discussed as an additional acceleration mechanism on the corrosion of carbon steel piping.

2. Experimental Procedures

2.1 Preparation of carbon steel and magnetite specimens

Carbon steel specimens were machined from SA106Gr.B pipe material into a size of 10 mm × 5 mm × 1 mm for electrochemical corrosion tests, and a size of 20 mm × 20 mm × 1 mm for immersion tests. The specimens were ground using silicon carbide papers down to grit 1000, and then ultrasonically cleaned in acetone.

Magnetite specimens were prepared by the electrodeposition of the magnetite layer on the whole surface of the carbon steel specimens described above. The electrodeposition solution consisted of 2 M NaOH, 0.1 M triethanolamine, and 0.043 M Fe₂(SO₄)₃. The electrodeposition process of magnetite was conducted at an applied potential of -1.05 V_{SCE} for 30 min at 80 °C in a three-electrode cell using a potentiostat. The detailed electrodeposition process of magnetite is given in previous studies [9,10]. Characteristics of the magnetite specimen were analyzed using a scanning electron microscope (SEM) and X-ray diffractometer.

2.2 Test solution

An alkaline aqueous solution of pH 9.5 at 25 °C was used in this work. The pH of the test solution was adjusted using ethanolamine, which is an organic chemical agent used to control the pH of secondary water in PWRs. All corrosion tests were carried out under a deaerated condition at 60 °C. For the deaerated condition, the test solutions were continuously purged with high-purity nitrogen gas (99.999%) at a flow rate of 100 cm³/min during testing. This test environment was designed to simulate a secondary water chemistry of PWRs.

2.3 Immersion corrosion test

Carbon steel coupons coupled and uncoupled to magnetite were used in the immersion corrosion test. In case of the coupled specimens, the area ratio (AR) of magnetite to carbon steel was controlled to be 1 and 20, respectively, as shown in Fig. 1. Four samples for each condition were exposed to the test solution for the weight loss measurement and surface analysis.

Fig. 2 shows the schematic of the test apparatus for the immersion corrosion test. The test apparatus consisted of a hot plate, water bath, specimen holder, and reaction flask equipped with a reflux condenser, sparger, overhead stirrer, and thermocouple. In order to

expose all specimens to the same fluid dynamic conditions, the samples were placed in each side of a regular dodecagon-shaped specimen holder, which is equidistant 6 cm from the center. After that, the specimen holder was loaded to the end of the overhead stirrer shaft and rotated at a rate of 320 rpm to make a fluid flow at the surface of specimens during the immersion corrosion test. When this angular velocity is converted into a linear velocity, the flow rate of the test solutions at the surface of the specimen is 2 m/s.

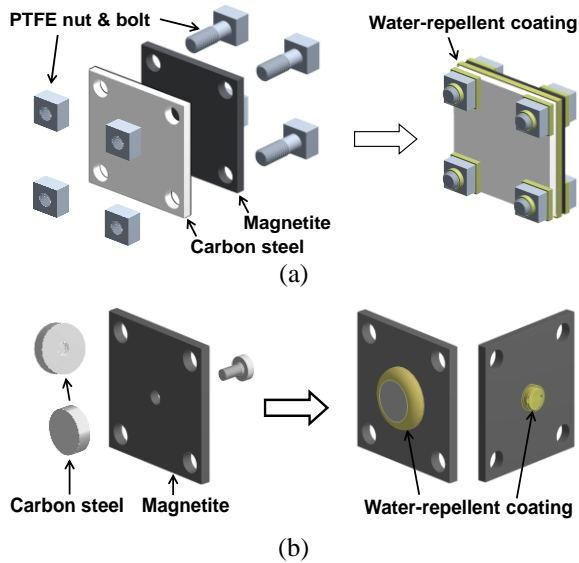


Fig. 1. Schematic for the preparation of the coupled specimens: (a) AR of 1 and (b) AR of 20.

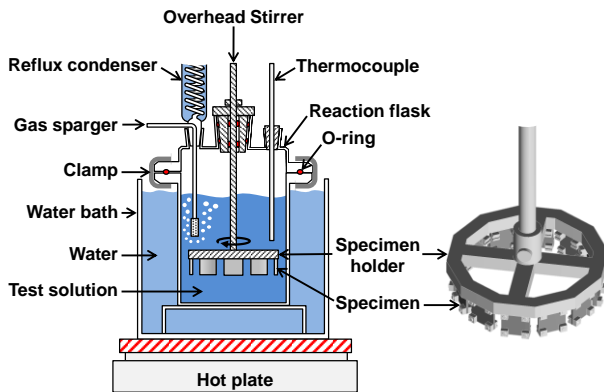


Fig. 2. Schematic of the test apparatus for the immersion corrosion test.

2.4 Electrochemical corrosion test

Potentiodynamic polarization tests were performed using a potentiostat and a three-electrode cell. A saturated calomel electrode and platinum wire were used as a reference and counter electrode, respectively. After the open circuit potential (OCP) was stabilized, polarization scans for carbon steel and magnetite were

started from 10 mV below the OCP to the anodic direction or from 10 mV above the OCP to the cathodic direction. The scan rate was 1 mV/s. Each anodic and cathodic polarization curve was finally combined in one graph.

3. Results and Discussion

Fig. 3 shows the weight change of carbon steel with and without coupling to magnetite after the immersion corrosion test in flowing test solutions at rate of 2 m/s at 60 °C for 500 h. Carbon steel both with and without coupling to magnetite indicated a weight loss. The weight loss of carbon steel uncoupled to magnetite was $0.14 \mu\text{g}/\text{cm}^2\text{h}$, while that was significantly increased by the galvanic coupling with magnetite. When the AR was 1, the weight loss of carbon steel was increased to $0.30 \mu\text{g}/\text{cm}^2\text{h}$. Furthermore, as the AR was increased to 20, the weight loss of carbon steel was drastically increased to $0.86 \mu\text{g}/\text{cm}^2\text{h}$. This result indicates that the galvanic coupling with magnetite accelerated the corrosion rate of carbon steel.

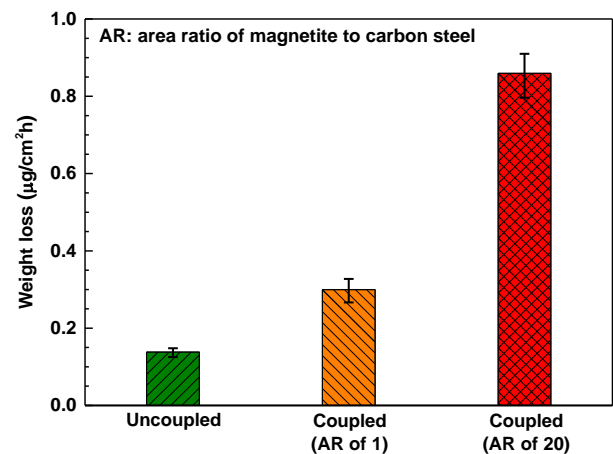


Fig. 3. Weight change of carbon steel with and without coupling to magnetite after the immersion corrosion test in flowing test solutions at a rate of 2 m/s at 60 °C for 500 h.

Fig. 4 shows the polarization curves of carbon steel and magnetite in stagnant and flowing test solutions. To evaluate the effect of the AR, polarization curves of magnetite with an area of 20 cm² were also presented in Fig. 4, which were calculated from those with an area of 1 cm².

In stagnant test solutions, the corrosion potential (E_{corr}) of carbon steel was about 300 mV lower than that of magnetite, as shown in Fig. 4(a). This means that carbon steel and magnetite will act as an anode and cathode, respectively, when these two materials are electrically connected. The anodic current density of carbon steel at the OCP was $1.35 \mu\text{A}/\text{cm}^2$. That is expected to increase to $8.06 \mu\text{A}/\text{cm}^2$ if equal areas of carbon steel and magnetite are galvanically coupled.

Furthermore, when the AR is increased to 20, the anodic current density of carbon steel will significantly increase to $21.04 \mu\text{A}/\text{cm}^2$.

In flowing test solutions, both the E_{corr} of carbon steel and magnetite were shifted in the positive direction compared to those in stagnant test solutions, as shown in Fig. 4(b). The overall polarization curves were also shifted in the direction of higher current density. The anodic current density of carbon steel at the OCP was increased from $1.35 \mu\text{A}/\text{cm}^2$ to $6.75 \mu\text{A}/\text{cm}^2$ by the fluid flow. Carbon steel still behaves as the anode of the galvanic couple with magnetite in flowing test solutions. Therefore, if carbon steel and magnetite are electrically connected, the extent of galvanic corrosion of carbon steel is expected to more increase than that in stagnant test solutions.

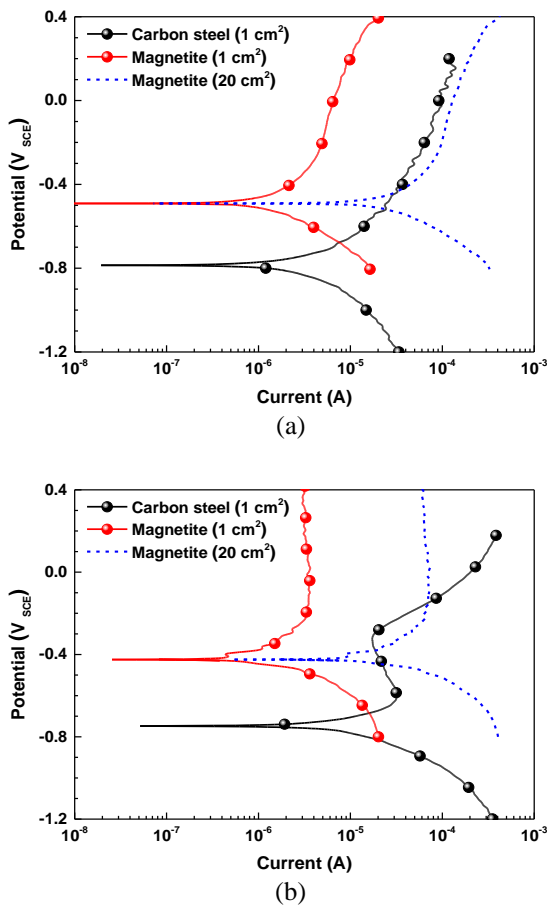


Fig. 4. Potentiodynamic polarization curves of carbon steel and magnetite in the test solutions at $60 \text{ }^\circ\text{C}$: (a) stagnant conditions and (b) flowing conditions.

In addition, the decrease of the anodic current in polarization curves of carbon steel scanned in flowing test solutions was observed in a specific potential range approximately from $-0.610 \text{ V}_{\text{SCE}}$ to $-0.320 \text{ V}_{\text{SCE}}$. These decrease may be caused by the anodic conversion of magnetite to hematite formed on carbon steel during the anodic polarization scan. This anodic conversion is

thermodynamically possible, because the stable phase of iron is hematite in a potential above about $-0.600 \text{ V}_{\text{SCE}}$ in the test solutions at $60 \text{ }^\circ\text{C}$ [11,12]. From the viewpoint of the electrical property, magnetite had a very small band gap of 0.1 eV , while hematite had a relatively large band gap of 2.2 eV [4]. That is, magnetite and hematite behave as a metal and semiconductor, respectively. Consequently, magnetite formed on carbon steel is rapidly converted to hematite in a flowing test solution than a stagnant test solution during the anodic polarization scan, and the semi-conductive character of these converted hematite will act as a barrier for the electrochemical reaction at the oxide/solution interface.

Based on the result of polarization tests, the accelerated corrosion of carbon steel by magnetite in Fig. 3 is caused by the fact that galvanic coupling with magnetite shifts the E_{corr} of carbon steel in the anodic direction and results in the increased corrosion current of carbon steel.

4. Conclusions

- (1) The weight loss of carbon steel was increased by the coupling with magnetite in flowing test solutions. Furthermore, a large area ratio of magnetite to carbon steel more increased the weight loss of carbon steel.
- (2) The electrochemical behavior of carbon steel and magnetite demonstrate that carbon steel acts as an anode of the galvanic couple with magnetite in both stagnant and flowing conditions, resulting in an increased corrosion current. This galvanic corrosion rate of carbon steel is expected to be increased by the fluid flow. Furthermore, that will more increase with increasing the AR.
- (3) Based on results of the electrochemical and immersion corrosion test, galvanic corrosion between carbon steel and magnetite is proposed as an additional acceleration factor on the corrosion of carbon steel piping in the secondary system of PWRs.

Acknowledgement

This work was supported by the National Research Foundation of Korea (NRF) grant funded by the Korea government (2017M2A8A4015159)

REFERENCES

- [1] F. N. Remy, M. Bouchacourt, Nucl. Eng. Des., Vol. 133, p. 23, 1992.
- [2] O. Jonas, Power, Vol. 129, p. 102, 1985.
- [3] R. B. Dooley, Int. J. Pres. Ves. Pip., Vol. 77, p. 85, 2000.

- [4] R. M. Cornell, U. Schwertmann, *The Iron Oxides: Structure, Properties, Reactions, Occurrences and Uses*, Wiley-VCH GmbH & Co. KGaA, Weinheim, pp. 117, 2003.
- [5] G. D. Song, S. H. Jeon, J. G. Kim, D. H. Hur, *Corrosion*, Vol. 72, p. 1010, 2016.
- [6] S. H. Jeon, G. D. Song, D. H. Hur, *Mater. Trans.*, Vol. 56, p. 1107, 2015.
- [7] S. H. Jeon, G. D. Song, D. H. Hur, *Mater. Trans.*, Vol. 56, p. 2078, 2015.
- [8] S. H. Jeon, G. D. Song, D. H. Hur, *Metals*, Vol. 5, p. 2372, 2015.
- [9] S. H. Jeon, G. D. Song, D. H. Hur, *Adv. Mater. Sci. Eng.*, Vol. 2016, Article ID 9038478, 2016.
- [10] S. H. Jeon, W. I. Choi, Y. H. Son, G. D. Song, D. H. Hur, *Coatings*, Vol. 6, 62, 2016.
- [11] W. Xu, K. Daub, X. Zhang, J.J. Noel, D. W. Shoesmith, J. C. Wren, *Electrochim. Acta.*, Vol. 54, p. 5727, 2009.
- [12] S. Nasrazadani, R. K. Nakka, D. Hopkins, J. Stevens, *Int. J. Pres. Ves. Pip.*, Vol. 86, p. 845, 2009.